Post-print version of the paper by Jingwen Wang et al. in ACS Sustainable Chem. Eng. 2018, 6, 9, 12025-12035. **DOI:** 10.1021/acssuschemeng.8b02321

Computer-aided Design of Ionic Liquids as Absorbent for Gas Separation Exemplified by CO_2 Capture Cases

Jingwen Wang,[†] Zhen Song,[‡] Hongye Cheng,[*,†] Lifang Chen,[†] Liyuan Deng, [§] Zhiwen Qi[*,†]

[†] *State Key Laboratory of Chemical Engineering, East China University of Science and Technology, 130 Meilong Road, 200237, Shanghai, China*

[‡] *Process Systems Engineering, Max Planck Institute for Dynamics of Complex Technical Systems, Sandtorstrasse 1, D-39106, Magdeburg, Germany*

[§] *Department of Chemical Engineering, Norwegian University of Science and Technology, Sem Sælandsvei 4, 7491 Trondheim, Norway*

[*]E-mail: hycheng@ecust.edu.cn, zwqi@ecust.edu.cn

ABSTRACT

In order to design ionic liquids as absorbents for gas separation, a systematic computer-aided ionic liquid design (CAILD) methodology is applied and demonstrated by three cases of CO_2 capture. Mixed-integer nonlinear programming (MINLP) problems are formulated, where a mass-based Absorption-Selectivity-Desorption index (*ASDI*) integrating the most important thermodynamic properties of ILs (i.e., gas solubility, selectivity, and desorption capacity) is proposed as the objective function and calculated by the COSMO-GC-IL inputted COSMO-SAC model. The physical properties of ionic liquids are implemented as optimization constraints, which are estimated by semi-empirical models. The reliability of the thermodynamic method for IL-gas systems is validated firstly by comparing a large number of

Post-print version of the paper by Jingwen Wang et al. in ACS Sustainable Chem. Eng. 2018, 6, 9, 12025-12035. **DOI:** 10.1021/acssuschemeng.8b02321

experimental and calculated data of Henry's law constant of different gases in ILs. Then, comparative CAILD studies are performed for CO_2 separation from flue gas (CO_2/N_2) to demonstrate the importance of *ASDI* for identifying practically attractive ILs. Afterwards, the developed method is applied to design IL solvents for the separation of CO_2 from syngas (CO_2/H_2) and sour gas (CO_2/H_2S). The correspondingly designed ILs for each case ($[OAc]^-$ and COOH-functionalized pyridinium for CO_2/H_2 and CO_2/N_2; $[AlCl_4]^-$ and long branched alkyl substituted pyridinium for CO_2/H_2S) are analyzed from the σ-profile point of view.

Keywords: Computer-aided ionic liquid design, Gas absorbent, MINLP, Absorption-Selectivity-Desorption index, CO_2 capture

Introduction

Ionic liquids (ILs) possess a set of unique properties, such as negligible vapor pressure, broad liquid range, and high chemical/ thermal stability. More importantly, the thermodynamic and physicochemical properties of ILs can be fine-tuned by judicious combination of cation, anion, and substitution groups to meet specific requirements in different tasks, making them "*designer solvents*".[1] Due to these attractive properties, ILs are widely expected as promising solvents for various chemical processes,[2-7] among which gas absorptions are extensively concerned.[8-12]

To ensure a technically and economically feasible IL-based gas absorption process, the selection of suitable IL absorbents is of the primary significance. For this purpose, however, the

Post-print version of the paper by Jingwen Wang et al. in ACS Sustainable Chem. Eng. 2018, 6, 9, 12025-12035. **DOI:** 10.1021/acssuschemeng.8b02321

experimental trial-and-error approach is expensive, time-consuming, and even unrealistic considering the huge library of possible cation-anion combinations. Therefore, computational screening or design of ILs based on reliable theoretical methods is highly desirable.[13]

Recently, studies on IL design employing the computer-aided molecular design (CAMD) approach, *i.e.*, computer-aided IL design (CAILD), have been continuously reported.[14-19] As demonstrated by these studies, CAILD reversely searches for the optimal IL structures to best meet the required target properties on the basis of quantitative structure-property relationship models.[20] That is to say, reliable predictive property models and suitable property criteria are two requisites in an effective CAILD. For gas absorption applications, the two requisites naturally lie in the thermodynamic model and the absorption performance index.

Until now, the UNIFAC model, which is widely used in CAMD,[21] has been successfully extended to IL-containing systems and used as the predictive thermodynamic method in CAILD by several researchers.[15,22-25] However, since such UNIFAC-IL model requires experimentally-fitted group interaction parameters, the current available parameter matrix is still far from adequate to cover the large variety of ILs and the huge diversity of IL-involved applications. In comparison to UNIFAC-IL, the COSMO-based activity coefficient models such as COSMO-RS [26-27] and COSMO-SAC[28-30] only require the quantum-chemically derived surface charge density profiles (σ-profile) and cavity volumes (V_{COSMO}) of molecules to predict the thermodynamic properties of pure-component fluids and fluid mixtures, including IL systems. Moreover, our very recent work has successfully developed a modified group contribution (GC) method for the prediction of σ-profiles and V_{COSMO} of ILs.[31] This COSMO-GC-IL model can

not only significantly reduce the computational cost to generate the required IL molecular information, but also well distinguish between IL structural isomers by considering the proximate effects. As the prerequisite to design IL absorbents, the fully predictive COSMO-SAC model combined with the computationally efficient COSMO-GC-IL method is of high potential for CAILD towards different gas separation tasks.

With respect to the other requisite for IL absorbents design, i.e., the absorption performance index, most previous studies on computational IL selection only concentrated on the capacity of ILs for the target gas components.[32-35] Recently, Farahipour et al.[36] and Zhao et al.[37] proposed that the selectivity towards different components in the gas mixture and the subsequent desorption capacity also play important roles in determining the applicability of IL absorbents. The above property parameters are all closely related to the practical absorption performance of ILs from different aspects. However, to the best of our knowledge, very scarce studies have considered all the above properties simultaneously or compared the effect of different target properties on IL selection. Moreover, since the molecular weights of different ILs may vary in a large range and are often much higher than those of conventional organic solvents, it is more straightforward to evaluate the separation performance of IL solvents on a mass basis from practical point of view.

Taking account of all the essential aspects mentioned above, a CAILD method with a mass-based Absorption-Selectivity-Desorption index (*ASDI*) integrating gas solubility, selectivity and desorption capacity is applied for designing ILs as gas absorbents in this contribution. The CAILD method and the mass-based performance index is validated by the flue gas (CO_2/N_2)

Post-print version of the paper by Jingwen Wang et al. in ACS Sustainable Chem. Eng. 2018, 6, 9, 12025-12035. **DOI:** 10.1021/acssuschemeng.8b02321

separation and then applied to another two important CO_2 separation tasks from syngas (CO_2/H_2) and sour gas (CO_2/H_2S). Finally, different designed results are compared and analyzed from the σ-profile point of view.

Methods

The whole computer-aided IL absorbents design method is structured in Fig. 1, which consists of four steps:

Step 1: Specify the target gas mixtures to be separated.

Step 2: Select IL group basis set. As the groundwork of the molecular design space, potential IL types are collected according to previous knowledge and experience on the given separation task.

Step 3: Formulate the MINLP problem for IL design by determining suitable objective function and necessary constraints. Any thermodynamic properties of interest can be employed as the objective function, while constraints on the structural feasibility and complexity as well as the key physical properties of ILs should be considered (as introduced in Sections 2.1 and 2.2, respectively). Specifically, the COSMO-SAC model with required inputs from the COSMO-GC-IL method is used for predicting thermodynamic properties and available semi-empirical models are adopted for estimating physical properties.

Step 4: Solve the MINLP problem to search for optimal IL solvents. Here, the combined simulated annealing (SA) and genetic algorithm (GA) extended by our previous work[38] is used since it merges the advantages of two algorithms to improve the searching ability towards

optimum solutions. The conceptual optimal algorithm maintains: (a) selecting chromosomes as parents from the random initial populations by the roulette wheel selection criterion; (b) applying crossover and mutation operator to produce new offspring and employing simulated annealing operator to decide whether the offspring remain; (c) decreasing the annealing temperature and exchanging information among populations if the exchange criterion is satisfied; (d) stopping the optimization or going back for loop until the stopping criterion is reached. For the cases studies in this work, the numbers of generations and individuals are 500 and 51, respectively; the probabilities for mutation and crossover operators are 0.08 and 0.7; the initial annealing temperature and annealing factor are set to 1.0×10^7 K and 0.985, which are all tuned accordingly after several tests to achieve a balance between outcome and computational consumption.

Objective functions for CAILD. As the designed ILs are novel and their chemical absorption potential cannot be exactly described, only physical absorption of gases is taken into account in the absorbent design in this work, which is widely employed in CAMD for gas separation processes.[35-37, 39]

General thermodynamic performance indices in absorption. The IL solubility for gases is directly related to the required solvent consumption and is therefore concentrated on by most previous reports. In dilute solutions, the gas solubility in a solvent is in reverse proportion to the Henry's law constant:

$$x_i = P_i / H_{i/s}(T) \qquad (1)$$

where P_i is the partial pressure of the gas above the solution; $H_{i/s}$ represents the Henry's law

Post-print version of the paper by Jingwen Wang et al. in ACS Sustainable Chem. Eng. 2018, 6, 9, 12025-12035. **DOI:** 10.1021/acssuschemeng.8b02321

constant of gas *i* in solution *s* and can be estimated as Eq. (2):

$$H_{i/s}(T) = \gamma_i^{\infty} P_i^s \quad (2)$$

In Eq. (2), γ_i^{∞} is the infinite dilution activity coefficient of the gas in the solution, which is calculated by COSMO-SAC in this work; P_i^s is the saturated vapor pressure of gas (see calculation details in Table S1, Supporting Information).

In addition to the solubility for target gas component, the absorption selectivity of IL is also very important, because practical gas absorption processes are commonly focused on dealing with multi-component gas mixtures rather than single component gases. The solvent selectivity towards target component *i* against other undesirable components *j* ($S_{i/j}$) is defined as:

$$S_{i/j} = \frac{H_{j/s}}{H_{i/s}} \quad (3)$$

Another important concern in gas absorption process is whether the subsequent desorption could be achieved elegantly for the sake of solvent reuse and energy saving. To this end, Farahipour et al.[36] proposed to evaluate the desorption capacity (*D*) of ILs as follows:

$$D = \frac{H^{abs}}{H^{des}} \quad (4)$$

where H^{abs} and H^{des} stand for the Henry's law constants at the assumed absorption and desorption temperature, respectively. Considering CO_2 absorptivity and the high heat capacity of ILs, the two temperatures are set at 298.15 K (ambient temperature) and 323.15 K in the following CO_2 capture case studies, respectively, which are most commonly used to screen or design IL solvents as CO_2 absorbents.[8,16,30,40]

Mass-based criteria for gas absorption design. Through the definitions in Eqs. (1) - (4), it can be found that the above thermodynamic performance indices are all based on the Henry's law constant of gases on a molar basis. That is to say, only the mole-based absorption performances of ILs are estimated. However, from a practical point of view, it is more desirable to select ILs with higher mass-based absorption performance. Moreover, when tackling practical separation tasks, different thermodynamic performance indices usually present contradictory dependencies on the solvents.[18,37,39] For instance, solvent with high absorption capacity may possess poor selectivity and/or desorption capacity, and vice versa. Thus, it is crucial to develop mass-based performance indices considering overall absorption performance.

For this purpose, a mass-based Absorption-Selectivity-Desorption index, *ASDI*, integrating the main thermodynamic properties of gas solubility, selectivity and desorption capacity is proposed to evaluate the overall absorption and desorption performance of IL candidates. Specifically, *ASDI* is defined as:

$$ASDI = H'_{i/s} \times \frac{1}{S'_{i/j}} \times D' \tag{5}$$

where H', S' and D' obtained as Eqs. (6) - (8) are the mass-based Henry's law constant, selectivity and desorption capacity, respectively.

$$H_{i/s}' = H_{i/s}(T) \times \frac{M_{\mathrm{IL}}}{M_i} \tag{6}$$

$$S_{i/j}' = \frac{H_{j/s}}{H_{i/s}} \times \frac{M_i}{M_j} \tag{7}$$

$$D' = D = \frac{H_{i/s}^{abs}}{H_{i/s}^{des}} \tag{8}$$

where M_{IL}, M_i, and M_j represent the molecular weights of IL, gas components *i* and *j*, respectively. It should be noted that the mass-based D' remains the same as the mole-based D.

From the definition of *ASDI*, it is clear that smaller values of H (H'), $1/S$ ($1/S'$) and D (D') of a component corresponds to higher solubility, selectivity, desorption capacity and hence a lower *ASDI* value is favorable for the gas separation.

Constraints for CAILD. *Structural constraints.* In the CAILD, IL structures are encoded as rooted trees which can guarantee the structural feasibility of ILs. Since a full description of this molecular encoding method is given in our earlier work,[38,41] only the major features are briefly introduced here. In a rooted tree structure of IL, cation core together with anion is regarded as the root node while substitutes attached to the cation core are leaf nodes grown on the root node. Each cation core and substitute node consists of four integer elements: node index, parent index, group ID, and group valence; anion codes contain only one elements corresponding to its ID (see the schematic exemplified by IL 1-(2-fluoro-2-hydroxypropyl)-3-propyl-imidazolium tetrafluoroborate in Fig. S1, Supporting Information). In addition to ensure the IL structural feasibility, the relative positions between groups can also be well recognized in this manner, which facilitates the prediction of IL σ-profiles and cavity volumes by the modified COSMO-GC-IL method and thereby enables further thermodynamic prediction by COSMO-SAC. Moreover, such a hierarchical data structure permits the complex manipulation of genetic operators so that the CAILD problem could be solved by the combined SA and GA algorithm.

The size and structural complexity of the designed ILs are limited by the constraints in Eqs. (9) - (11):

Post-print version of the paper by Jingwen Wang et al. in ACS Sustainable Chem. Eng. 2018, 6, 9, 12025-12035. **DOI:** 10.1021/acssuschemeng.8b02321

$$\sum_{i \in Sub} n_i \le n_{Sub}^U \tag{9}$$

$$\sum_{i \in C,CH} n_i \le n_{C,CH}^U \tag{10}$$

$$\sum_{i \in Sub^*} n_i \le n_{Sub^*}^U \tag{11}$$

where i and n_i refer to the group ID and the occurrence frequency of group i of substituents listed in Table 1; *Sub* stands for the subset of substituent groups, while *Sub** represents the subset of functional substituent groups (i.e., substituent groups except for CH_3, CH_2, CH, C). Eq. (9) limits the overall size of IL molecule with an upper bound (n_{Sub}^U) on the number of substitutes; Eq. (10) restricts the number of branch chain structures ($n_{C,CH}^U$) and Eq. (11) imposes an upper bound ($n_{Sub^*}^U$) on the number of functional substitutes. By definition, these limitations on group numbers can be properly relaxed according to different requirements.

Physical property constraints. To ensure that the designed IL could act as liquid absorbents under common operating conditions and have relatively low viscosity (η), the physical properties of ILs are constrained as follows.

$$T_m \le 298.15\,K \tag{12}$$

$$\eta \le 100\,\mathrm{c}P \tag{13}$$

For the estimation of melting point (T_m) of ILs, the GC model developed by Lazzús[42] is used:

$$T_m = 288.7 + \sum_{i=1}^{Ca,sub} n_i \Delta t_{ci} + \sum_{j=1}^{An} n_j \Delta t_{aj} \tag{14}$$

where n_i and n_j are the occurrence of the groups i and j in the IL, Δt_{ci} and Δt_{ai} are the

contribution of the cation group *i* and the anion group *j* to the T_m. The viscosity of ILs is calculated by a GC-based feed-forward artificial neural network (FFANN) model.[43] Both the two above methods are parametrized from a large number of experimental data and have been proven to be reliable prediction tools for estimating IL physical properties in IL selection.[18,25,35,38,39]

Method validation

Thermodynamic model validation for IL-gas systems. Since thermodynamic property prediction is the prerequisite to design IL absorbent, the reliability of the thermodynamic method should be evaluated beforehand. As mentioned above, the COSMO-SAC model inputted from COSMO-GC-IL is employed for predicting thermodynamic properties in CAILD. This method has been demonstrated to be able to accurately predict the activity coefficients of different organic solutes in ILs as well as liquid-liquid equilibria of IL-involved polar and non-polar systems.[31] Here, the prediction ability of the method for different IL-gas systems is further evaluated.

Firstly, COSMO-SAC predictions on the Henry's law constants of different gases in ILs inputted from the COSMO-GC-IL method are compared to those directly inputted from DMol^3 calculation (i.e., the DMol^3 module in the Accelrys Materials Studio 6.1 software package).[44] The involved gases cover not only those relevant to different CO_2 capture occasions, such as CO_2, N_2, H_2, and H_2S, but also those widely studied C_1 - C_4 hydrocarbons (CH_4, C_2H_2, C_2H_4, C_2H_6, C_3H_8, C_4H_6, C_4H_8, and C_4H_{10}). The studied ILs are also of different characteristics of

Post-print version of the paper by Jingwen Wang et al. in ACS Sustainable Chem. Eng. 2018, 6, 9, 12025-12035. **DOI:** 10.1021/acssuschemeng.8b02321

cation and anion types (see the detailed data in Table S2 - S6, Supporting Information). As depicted in Fig. 2a, the predictions in these two cases are in very close agreement. The average relative deviation (*ARD*) between them is evaluated by:

$$ARD = \frac{1}{N}\left(\sum \frac{\left| H_{i/s}^{\ DMol^3} - H_{i/s}^{\ COSMO-GC-IL} \right|}{H_{i/s}^{\ DMol^3}} \right) \times 100\% \qquad (15)$$

where N is the total number of data points. The *ARD* for the total 835 data points in this comparison is only 3.83%. This fact demonstrates that the employed COSMO-GC-IL is an accurate input method for the COSMO-SAC model for estimating thermodynamic properties of IL-gas systems.

Furthermore, the predicted Henry's law constants in the above data set are further compared to the experimental data. As seen in Fig. 2b, the predicted data are basically evenly located in a small range close to the diagonal. From a quantitative point of view, over 73% of these 835 data points present a relative deviation lower than 20%, resulting in a total *ARD* of 15.63%. Therefore, the COSMO-GC-IL inputted COSMO-SAC method can be employed as a reliable tool for predicting the thermodynamic properties in CAILD of gas absorbents.

Objective function validation with the flue gas separation case study. In CAILD, the target properties in the objective function also play a crucial role in the practical applicability of final selected ILs. However, in previous literature, the effect of different target properties on IL selection was scarcely compared and no CAILD has employed the proposed *ASDI* as the objective function. Therefore, in this section, the importance and suitability of *ASDI* for designing practically applicable IL absorbents are addressed by the case study on the flue gas

Post-print version of the paper by Jingwen Wang et al. in ACS Sustainable Chem. Eng. 2018, 6, 9, 12025-12035. **DOI:** 10.1021/acssuschemeng.8b02321

separation. The post-combustion flue gas separation is the most widely studied CO_2 capture scenario, where the flue gas could be roughly modelled as a CO_2/N_2 mixture with the CO_2 mole fraction of 3% - 15%.[39-40]

To demonstrate the importance of the proposed *ASDI*, comparative CAILD based on different objective functions, namely *H*, *H'*, *1/S'*, *D'* and *ASDI*, are performed. All the groups in Table 1 are selected as the group basis set for CAILD, and the conditions for absorption are set at 298.15 K and atmospheric pressure. The CAILD tasks can be generally expressed as:

$$\text{min.} \quad f_{obj} \quad (f_{obj} = H, H', 1/S', D', ASDI)$$

s.t.

Chemical complexity constraints:

$$\sum_{i \in Sub} n_i \leq 35 \tag{16}$$

$$\sum_{i \in C,CH} n_i \leq 2 \tag{17}$$

$$\sum_{i \in Sub^*} n_i \leq 1 \tag{18}$$

Physical property constraints: Eqs. (12) - (13).

In a typical run to solve the above MINLP, an initial population of 51 individuals is constructed and the evolution process is then carried out for maximum 500 generations to search for the optimal IL structures that best satisfy the objective function. The top 10 IL candidates based on each objective function are obtained, and their detailed information is given in Tables S7 - S11 (Supporting Information). To directly compare the effects of different objective functions, the absorption performance indices of the top 10 designed ILs in each case are

summarized in Table 2. As seen, the performance indices of the obtained ILs in different cases vary in a notable range. From entries 1 and 2, the IL candidates identified by *H* certainly have lower mole-based Henry's law constants than those identified by *H′*; nevertheless, their mass-based Henry's law constants are around 2 times of those in the latter case due to the much higher molecular weights. It indicates that the ILs directly identified by *H′* have a higher mass-based absorption capacity and thus are more attractive from the practical point of view. Such a comparison clearly demonstrates the significance of employing mass-based absorption performance indices in the objective function.

As compared in entries 2 - 4, although the lowest values of each individual performance indices are obtained when using it as the objective function, the values of other indices vary significantly for the designed ILs in different cases. For example, when *1/S′* is employed as the objective function, the designed ILs possess the lowest *1/S′* of 0.017 - 0.024 among all these CAILD tasks; however, their *H′* and *D′* are 293.62 - 2369.31 and 0.52 - 0.61, respectively, which are much higher compared to the ILs identified in other two cases. By comparison, the ILs identified by the combined performance index *ASDI* not only reach the lowest *ASDI* (0.89 - 1.04, see entry 5), but also have satisfactory *H′*, *1/S′*, and *D′* (see entries 2 - 4). Therefore, it can be concluded that the proposed *ASDI* is an effective index to make a trade-off among all the desired properties in CAILD.

In order to evaluate the correlation between the *ASDI* and process property and further demonstrate the efficiency of the *ASDI* for designing practical ILs, the energy consumption of the best candidates in each generation are calculated based on the absorption process proposed

by Zhang et al.[40] The detailed description on how to calculate the energy consumption of ILs is given in Table S12 (Supporting Information). As illustrated in Fig S2 (Supporting Information), with the population develops, the energy consumption of the designed IL candidates based on *ASDI* decrease from the first generation and finally converge to the lowest value. It is noticeable that the tendency of energy consumption change almost keeps pace with that of the *ASDI*. Furthermore, the optimal designed IL [MPy13$(CH_2)_2$COOH][OAc] based on *ASDI* also exhibit the lowest energy consumption values (Table S12, Supporting Information). All these results demonstrate the suitability of the proposed *ASDI* for IL absorbents design for CO_2 capture.

Optimization process for flue gas separation. For the flue gas separation case, the optimization processes for *H*-based and *ASDI*-based MINLP are tracked in Fig. 3 with the structure of the best IL candidate of the numbered generation. As illustrated in Fig. 3a, the *H*-based optimization process shows that the structural evolution is relatively unstable, where the structure of IL changes significantly with the evolution of generation. The IL with longer branched alkyl substitute is favorable to meet a lower *H* on a molar basis. At the maximum 500 generation, the optimal IL is [$P_{1,2,18}(CH_2)_2CO(CH_2)_{10}CH_3$][$Tf_2N$], whose structure has very long branched alkyl chains and even reaches the upper bound of the number of substitutes. It is unrealistic to employ such IL with huge molecular weight in gas absorption process.

Compared to the *H*-based optimization process, the *ASDI*-based optimization process is more practicable, as shown in Fig. 3b. The structural evolution in *ASDI*-based optimization process is relatively stable that the IL structure remains unchanged from earlier generation. In addition, the molecular weight of designed ILs is much smaller due to the shorter branched

alkyl substitutes. As demonstrated, the best IL for the first 29 generations are [DMP]-based ILs with carboxyl attached to tetraalkylphosphonium skeleton. Then $[OAc]^-$ anion emerged at the 30th generation with the *ASDI* value decreasing from 3.37 to 2.21. After that, the cation core is shown to be pyridinum from the 101th generation while the anion remains unchanged till the last generation. Correspondingly, the objective values decrease smoothly from 2.21 to 1.5 and finally converge to 0.89 after the 177th generation. The top 10 designed absorbents are all [OAc]-based ILs paired with a COOH-functionalized pyridinium cation (see Table S11, Supporting Information), among which [MPy13$(CH_2)_2$COOH][OAc] is the optimal. This suggests two valuable ways to enhance the post-combustion CO_2 capture ability of ILs, *i.e.*, employing $[OAc]^-$ anion and functionalizing the cation with COOH group, which agree well with the previous experimental data and theoretical studies.[36,39,45,46,47,48]

To further demonstrate the high potential of the designed ILs, the absorption performances of the top 10 designed ILs are compared to $[P_{4,4,4,10}]$[DCA], which is reported as the optimal IL absorbent in a very recent CAILD study.[35] As shown in Fig. 4a, the H' of $[P_{4,4,4,10}]$[DCA] (139.52) is about 2 times compared to that of the designed 10 ILs (60.11 -70.57); meanwhile, the $1/S'$ and D' of $[P_{4,4,4,10}]$[DCA] are also notably higher as shown in Fig. 4b and Fig. 4c, which finally result in a significantly higher *ASDI* (see Fig. 4d). In addition, when the amount of CO_2 desorbed from the top of the stripper is set to be 1 mol, the energy consumption of the optimal IL in this work is 0.3082 MJ, which is only 80% of the corresponding consumption of the $[P_{4,4,4,10}]$[DCA] (0.3902 MJ). In other words, the ILs designed here outperform $[P_{4,4,4,10}]$[DCA] from all the considered aspects. This again verifies the suitability of the proposed *ASDI* for

identifying practically attractive IL absorbents.

Application for syngas and sour gas treatment

In addition to the flue gas separation, the CO_2 separation from syngas and sour gas are another two important CO_2 capture scenarios. However, as far as we concern, very few experimental or simulation studies have particularly focused on using ILs for these two separations.[12,49,50] Therefore, after validating the effectiveness of the proposed CAILD method, two more case studies are carried out for these two applications.

CO_2 separation of syngas. The treatment of syngas is also well-known as pre-combustion CO_2 capture, which deals with the CO_2/H_2 mixtures generated from the coal gasification or natural gas reformation. For the CAILD in this case, the MINLP problem is formulated as:

min. *ASDI*

s.t.

Chemical complexity constraints: Eqs. (16) - (18)

Physical property constraints: Eqs. (12) - (13)

Through the solution of the MINLP, the top 10 ILs together with their predicted absorption performance indices are obtained and listed in Table 3. As seen, these ILs are all of very similar structures as those obtained in the CO_2/N_2 case, that is to say, a $[OAc]^-$ anion paired with a COOH-functionalized pyridinium cation. Specifically, the top 2 ILs [MPy13CH_2COOH][OAc] and [MPy13$(CH_2)_2$COOH][OAc] in this case also rank as the second and first among the top 10 ILs in the CO_2/N_2 case, respectively. Such similarity can be further observed in the

optimization process shown in Fig. 5, where the anions of the best candidates also change from the $[DMP]^-$ to $[OAc]^-$ after the 26th generation.

In the CO_2/H_2 case, the *ASDI* of the top 10 ILs lies in the range of [0.013, 0.022], with each of the individual performance criterion within the range as follows: H' (60.11 - 84.49), $1/S'$ (0.00053 - 0.00056), and D' (0.41 - 0.49). To demonstrate the high potential of the designed ILs, the optimal IL $[MPy13CH_2COOH][OAc]$ is compared to [BMIM][TfO], which is experimentally reported by Liu et al.[51] as a very promising absorbents for CO_2/H_2 separation with high CO_2 solubility and selectivity. As listed in Table 3, the H', $1/S'$, and D' of $[MPy13CH_2COOH][OAc]$ are 61.99, 0.00053, and 0.41, which are only 25.4%, 48.2%, and 75.9% of those predicted for [BMIM][TfO], respectively. The much higher absorption performances from all the three aspects indicate the practically potential of the designed ILs.

CO_2 separation of sour gas. In industry, CO_2 and H_2S are always removed simultaneously from refinery gas streams, coal-fired or petroleum-burning power plant, natural gas streams, and so on. This brings about a large amount of sour gas mixture of CO_2 and H_2S, which needs to be separated for further use.[33,34,52] To design ILs for this separation, a MINLP problem is formulated in the same manner as in the syngas separation case study.

In this CAILD case, the objective value of the best chromosome in each generation is demonstrated in Fig. 6. The best IL candidates of the first 22 generations have a $[H_2PO_4]^-$ anion and an imidazolium cation skeleton with the objective value of 7.76 - 10.17. Then the objective value drops to 6.49 at the 23th generation and the anion is replaced by $[Tf_2N]^-$. From generation 23 to generation 190, the objective value decreases smoothly from 6.49 to 6.02 with the anion

unchanged. As the evolution of population going on, $[Tf_2N]^-$ anion is replaced with $[AlCl_4]^-$ at the 191th generation with objective value of 4.17. Then the pyridinium cation core supersedes the previous one at the 202th generation. Finally, the objective value converges to 3.56 after 336 generations.

The detailed information of the top 10 designed ILs is provided in Table 4. As seen, these ILs are all combinations of $[AlCl_4]^-$ anion and long branched alkyl substituted pyridinium cation, which are completely different from those obtained in the CO_2/N_2 and CO_2/H_2 cases. To evaluate the potential of the designed ILs, [BMIM][$MeSO_4$] is employed as a benchmark solvent due to its higher CO_2/H_2S selectivity.[52] By comparison, all the top 10 ILs outperform [BMIM][$MeSO_4$] from the three aspects of *H'*, *1/S'*, and *D'*; consequently, the *ASDI* of [BMIM][$MeSO_4$] (8.64) are 1.81 - 2.43 times high as the designed ILs (3.56 - 4.75). It suggests that the designed ILs are indeed more promising solvents for CO_2/H_2S separation from the practical point of view.

Analysis of designed results from σ-profile perspective

As discussed above, the top IL candidates for CO_2/N_2 and CO_2/H_2 separation are of very similar structures whereas those obtained in the CO_2/H_2S case are completely different. To better understand such results, the characteristics of the different CO_2 capture tasks and the correspondingly designed ILs are interpreted from the σ-profile theoretical point of view. Specifically, the σ-profiles of the gas components and the optimal IL candidates are analyzed.

σ-Profile is the most important molecule-specific properties in the COSMO-based theory,

which characterizes the electrostatic polarity and charge distribution of a molecule (Lin and Sandler, 2002; Lee and Lin, 2015). The whole σ range can be divided into three different regions, namely the nonpolar region (-0.0084 e/Å^2 $< \sigma <$ 0.0084 e/Å^2), the hydrogen-bond (HB) donor region ($\sigma < -0.0084$ e/Å^2) and the hydrogen-bond (HB) acceptor region ($\sigma >$ 0.0084 e/Å^2). Generally, a broader distribution and/or high peaks of σ-profile outside the nonpolar region indicate a higher polarity of the molecule. From Fig. 7a, the σ-profiles of CO_2, N_2, and H_2 are generally located in the nonpolar region, which corresponds to their highly non-polar feature. Nevertheless, their non-polarity can still be ranked as such: $CO_2 < N_2 < H_2$, according to the breadth of their σ-profiles. For H_2S, in addition to a wide distribution in the nonpolar region, pronounced peaks in the HB donor and HB acceptor regions are also observed, demonstrating its strong polarity.

Due to the close non-polarity of N_2 and H_2 gas molecules, the suitable ILs for CO_2 captures from flue gas and syngas are of high similarity, which could well account for the very similar structures identified by CAILD in the two cases. To capture CO_2 from flue gas and syngas, relatively polar ILs are required to ensure a high selectivity towards N_2 and H_2 as CO_2 is the more polar gas in the mixture. This agrees well with the designed ILs based on $[OAc]^-$ anion and COOH-functionalized pyridinium cation, which both have a strong polarity. As seen in Figs. 7b and 7c, the $[OAc]^-$ anion has a high peak in the HB acceptor region (around 0.02 e/Å^2) while the COOH-functionalized pyridinium cation possesses a notable peak in both the HB donor and HB acceptor region. On the contrary, to capture CO_2 from sour gas, non-polar ILs are desired as CO_2 turns to be the more nonpolar compared to H_2S. Consequently, the designed ILs are

composed of long alkyl substituted pydinium cation combined with $[AlCl_4]^-$ anion, whose strong non-polarity can also clearly illustrated by their σ-profiles (see Figs. 7b and 7c, respectively).

Conclusion

A systematic CAILD method with a mass-based Absorption-Selectivity-Desorption index (*ASDI*) for IL absorbents design is developed and exemplified by three CO_2 capture cases. The Henry's law constants predicted by the COSMO-GC-IL inputted COSMO-SAC model is proven to be reliable. Through the comparative CAILD for the flue gas separation, the integrated *ASDI* is demonstrated to be able to identify practically promising ILs absorbents by reaching a good trade-off among different desired thermodynamic properties and giving rise to low energy consumption. The proposed method is further applied to other CO_2 capture cases of syngas and sour gas separation. It is found that the top 10 ILs for the flue gas and syngas separation are all combinations of $[OAc]^-$ and COOH-functionalized pyridinium cation whereas those for the sour gas treatment are composed of $[AlCl_4]^-$ and long branched alkyl substituted pyridinium cation. The difference of design results for the three CO_2 capture tasks are attributed to the key role of the relative polarity of CO_2 in the gas mixture. The proposed CAILD method could be easily extended to other gas absorption applications to design or select alternative absorbents.

List of symbols

x_i composition of component *i* in liquid

P_i partial pressure of component *i*, bar

$H_{i/s}$ Henry's law constant of gas *i* in solvent *s*, bar

T temperature, *K*

γ_i^{∞} infinite dilution activity coefficient of gas *i*

P_i^s saturated vapor pressure of gas *i*, bar

$S_{i/j}$ selectivity of component *i* against component *j*

D desorption capacity

H^{abs} Henry's law constant at assumed absorption temperature, bar

H^{des} Henry's law constant at assumed desorption temperature, bar

$ASDI$ Absorption-Selectivity-Desorption index, bar

$H'_{i/s}$ mass-based Henry's law constant of gas *i* in solvent *s*, bar

$S'_{i/j}$ mass-based selectivity of component *i* against component *j*

D' mass-based desorption capacity

M molecular weight

n_i occurrence frequency of group *i*

n_{Sub}^U upper bound of substituents

$n_{C,CH}^U$ upper bound of group C and CH

$n_{Sub^*}^U$ upper bound of functional substituents

T_m melting point, K

η viscosity, cP

Δt_{ci} melting point contribution of cation group *i*, K

Post-print version of the paper by Jingwen Wang et al. in ACS Sustainable Chem. Eng. 2018, 6, 9, 12025-12035. **DOI:** 10.1021/acssuschemeng.8b02321

Δt_{ai} melting point contribution of anion group *i*, K

σ surface screening charge density, e/Å^2

$P(\sigma)$ surface area with a charge density of σ, Å^2

Abbreviations

$[P_{1,2,18}(CH_2)_2CO(CH_2)_{10}CH_3][Tf_2N]$

methyl-ethyl-octadecyl-3-tetradecanone bis(trifluoromethylsulfonyl)imide

$[DMP]^-$ dimethyl phosphate

$[OAc]^-$ acetate

$[MPy13(CH_2)_2COOH][OAc]$ 1-methyl-3-propionyloxy acetate

$[P_{4,4,4,10}][DCA]$ tributyl(decyl)phosphonium dicyanamide

$[MPyCH_2COOH][OAc]$ 1-methyl-3-carbethoxy-acetate

[BMIM][TfO] 1-butyl-3-methylimidazolium triflate

$[H_2PO_4]^-$ dihydrogenphosphate

$[Tf_2N]^-$ bis(trifluoromethylsulfonyl)imide

$[AlCl_4]^-$ tetrachloroaluminate

$[BMIM][MeSO_4]$ 1-butyl-3-methylimidazolium methylsulphate

Associated content

Supporting information

Supporting information associated with this article can be found in the online version at http://dx.doi.org/10.1016***.

Post-print version of the paper by Jingwen Wang et al. in ACS Sustainable Chem. Eng. 2018, 6, 9, 12025-12035. **DOI:** 10.1021/acssuschemeng.8b02321

Acknowledgement

This research is supported by the National Natural Science Foundation of China (21576081, 21776074), Shanghai Committee of Science and Technology (16dz1206203), PetroChina Innovation Foundation, and 111 Project (B08021).

References

(1) Brennecke, J. F.; Maginn, E. J.. Ionic liquids: innovative fluids for chemical processing. *AIChE J*. **2001**, 47, 2384-2389 DOI 10.1002/aic.690471102.

(2) Giovanoglou, A.; Barlatier, J.; Adjiman, C. S.; Pistikopoulos, E. N.; Cordiner, J. L. Optimal solvent design for batch separation based on economic performance. *AIChE J*. **2003**, 49, 3095-3109 DOI 10.1002/aic.690491211.

(3) Freire, M. G.; Claudio, A. F. M.; Araujo, J. M. M.; Coutinho, J. A. P.; Marrucho, I. M.; Lopes, J. N. C. et al. Cheminform abstract: Aqueous biphasic systems: a boost brought about by using ionic liquids. *Cheminform* **2012**,*43*(41), 4966-4995. DOI 10.1002/chin.201241265

(4) Qin, L.; Zhang, J. N.; Cheng, H. Y., Chen, L. F., Qi, Z. W, Yuan, W. Selection of imidazolium-based ionic liquids for vitamin e extraction from deodorizer distillate. *ACS Sustainable Chem. Eng*. **2015**, *2*(2), 583 - 590 DOI 10.1021/acssuschemeng.5b01330.

(5) Song, Z.; Zhang, J. J.; Zeng, Q.; Cheng, H. Y.; Chen, L. F.; Qi, Z. W. Effect of cation alkyl chain length on liquid-liquid equilibria of {ionic liquids+ thiophene+ heptane}: COSMO-RS prediction and experimental verification. *Fluid Phase Equilib*. **2016**, 425, 244-251 DOI 10.1016/j.fluid.2016.06.016.

(6) Martins, M. A. R.; Domańska, U.; Schröder, B.; Coutinho, J. A. P.; Pinho, S. P. Selection of ionic liquids to be used as separation agents for terpenes and terpenoids. *ACS Sustainable*

Chem. Eng. **2016***, 4*(2), 548-556 DOI 10.1021/acssuschemeng.5b01357.

(7) Zheng, S. S.; Nie, Y.; Zhang, S. J.; Zhang, X. P.; Wang, L. J. Highly efficient dissolution of wool keratin by dimethylphosphate ionic liquids. *ACS Sustainable Chem. Eng.* **2015**, 3, 2925 DOI: 10.1021/acssuschemeng.5b00895.

(8) Zhang, X. C.; Liu, Z. P.; Wang, W.C. Screening of ionic liquids to capture CO_2 by COSMO-RS and experiments. *AIChE J.* **2008,** 54, 2717-2728, DOI 10.1002/aic.11573.

(9) Chau, J.; Obuskovic, G.; Jie, X.; Mulukutla, T.; Sirkar, K. K. Solubilities of CO_2 and helium in an ionic liquid containing poly(amidoamine) Dendrimer Gen 0. *Ind. Eng. Chem. Res.* **2013**, 52, 10484-10494 DOI 10.1021/ie303426q.

(10) Zhao, X.; Yang, Q. W.; Xu, D.; Bao, Z. B.; Zhang, Y.; Su, B. G.; Ren, Q. L.; Xing, H. B. Design and screening of ionic liquids for C_2H_2/C_2H_4 separation by COSMO-RS and experiments. *AIChE J.* **2015**, 61, 2016-2027 DOI 10.1002/aic.14782.

(11) Liu, X. Y.; Huang, Y.; Zhao,Y.S.; Gani, R.; Zhang, X.P.; Zhang, S.J. Ionic liquid design and process simulation for decarbonization of shale gas. *Ind. Eng. Chem. Res.* **2016**, 55, 5931-5944 DOI 10.1021/acs.iecr.6b00029.

(12) Zeng, S. J.; Zhang, X. P.; Lu, B.; Zhang, X. C.; Wang, H.; Wang, J. J.; Bao, D.; Li, M. D.; Liu, X. Y.; Zhang, S. J. Ionic-liquid-based CO_2 capture systems: structure; interaction and process. *Chem. Rev.* **2017**, 117(14), 9625-9673 DOI 10.1021/acs.chemrev.7b00072.

(13) Song, Z.; Zhou, T.; Zhang, J. N.; Cheng, H. Y.; Chen, L. F.; Qi; Z. W. Screening of ionic liquids for solvent-sensitive extraction - with deep desulfurization as an example. *Chem. Eng. Sci.* **2015**, 129; 69-77 DOI 10.1016/j.ces.2015.02.023.

(14) Mcleese, S. E.; Eslick, J. C.; Hoffmann, N. J.; Scurto, A.M.; Camarda, K.V. Design of ionic liquids via computational molecular design. *Comput. Chem. Eng*. **2010**, 34(9), 1476-1480 DOI 10.1016/j.compchemeng.2010.02.017.

(15) Roughton, B. C.; Christian, B.; White, J.; Camarda, K. V.; Gani, R. Simultaneous design

of ionic liquid entrainers and energy efficient azeotropic separation processes. *Comput. Chem. Eng.* **2012**, 42, 248-262 DOI 10.1016/j.compchemeng.2012.02.021.

(16) Karunanithi, A. T.; Mehrkesh, A. Computer-aided design of tailor-made ionic liquids. *AIChE J*. **2013**, 59, 4627-4640 DOI 10.1002/aic.14228.

(17) Song, Z.; Zhou, T.; Qi, Z. W.; Sundmacher K. Systematic method for screening ionic liquids as extraction solvents exemplified by an extractive desulfurization process. *ACS Sustainable Chem. Eng.* **2017**, 5(4), 3382-3389. DOI 10.1515/chempap-2015-0016

(18) Scheffczyk, J.; Fleitmann, L.; Schwarz, A.; Lampe, M.; Bardow, A.; Kai, L. COSMO-CAMD: a framework for optimization-based computer-aided molecular design using COSMO-RS. *Chem. Eng. Sci*. **2016**, 159. DOI 10.1016/j.ces.2016.05.038

(19) Scheffczyk, J.; Fleitmann, L.; Schwarz, A.; Bardow, A.; Kai, L. Computer-aided molecular design by combining genetic algorithms and COSMO-RS. *Comput.-Aided Chem. Eng*. **2016**, 38, 115-120 DOI 10.1016/b978-0-444-63428-3.50024-2.

(20) Gardas, R. L.; Coutinho, J. A. P. Applying a QSPR correlation to the prediction of surface tensions of ionic liquids. *Fluid Phase Equilib.* **2008**, *265*(1–2), 57-65 DOI 10.1016/j.fluid.2008.01.002.

(21) Gani, R.; Brignole, E. A. Molecular design of solvents for liquid extraction based on UNIFAC. *Fluid Phase Equilib*. **1983**, 13(83), 331-340. DOI 10.1016/0378-3812(83)80104-6.

(22) Lei, Z. G.; Dai, C. N.; Liu, X.; Li, X.; Chen, B. H. Extension of the UNIFAC model for ionic liquids. *Ind. Eng. Chem. Res.* **2012**, 51(37), 12135-12144 DOI 10.1021/ie301159v.

(23) Lei, Z. G.; Zhang, J. G.; Li, Q. S.; Chen, B. H. UNIFAC model for ionic liquids. *Ind. Eng. Chem. Res.***2014**, 48(5), 2697-2704 DOI 10.1021/ie801496e.

(24) Lei, Z. G.; Dai, C. N.; Zhu, J. Q.; Chen, B. H. Extractive distillation with ionic liquids: a

review. *AIChE J.* **2014**, 60, 3312-3329 DOI 10.1002/aic.14537.

(25) Song, Z.; Zhang, C.; Qi, Z. W.; Zhou, T.; Sundmacher, K. Computer-aided design of ionic liquids as solvents for extractive desulfurization. *AIChE J.* **2017**, 64 (3), 1013-1025. DOI 10.1002/aic.15994.

(26) Klamt, A.; Jonas, V.; Bürger, T.; Lohrenz, J. C. W. Refinement and parameterization of COSMO-RS. *J. Phys. Chem. A.* **1998**, 102(26), 5074-5085 DOI 10.1016/b9-78-044451-9/94850-0079.

(27) Klamt, A.; Eckert, F.; Arlt, W. COSMO-RS: an alternative to simulation for calculating thermodynamic properties of liquid mixtures. *Annu. Rev. Chem. Biomol. Eng.* **2010**, 1(1), 101-122 DOI 10.1146/annurev-chembioeng-073009-100903.

(28) Lin, S. T.; Sandler, S. I. A Priori Phase Equilibrium Prediction from a Segment Contribution Solvation Model. *Ind. Eng. Chem. Res.* **2002**, 41(5), 899-913 DOI 10.1021/ie0308689.

(29) Wang, S.; Sandler, S. I.; Chen, C. C. Refinement of COSMO-SAC and the applications. *Ind. Eng. Chem. Res.* **2015**, 47, 1-15 DOI 10.1021/ie070465z.

(30) Lee, B. S.; Lin, S. T. Screening of ionic liquids for CO_2 capture using the COSMO-SAC model. *Chem. Eng. Sci.* **2015**, 121,157-168 DOI 10.1016/j.ces.2014.08.017.

(31) Zhang, J. N.; Peng, D. L.; Song, Z.; Zhou, T.; Cheng, H. Y.; Chen, L. F.; Qi, Z. W. COSMO-descriptor based computer-aided ionic liquid design for separation processes. Part I: Modified group contribution methodology for predicting surface charge density profile of ionic liquids. *Chem. Eng. Sci.* **2017**, 162, 355-363 DOI 10.1016/j.ces.2014.08.017.

(32) Anthony, J. L.; Anderson, J. L.; Maginn, E. J.; Brennecke, J. F. Anion effects on gas solubility in ionic liquids. *J. Phys. Chem. A.* **2005**, 109, 6366-6374 DOI 10.1021/jp046404l.

(33) Mortazavi-Manesh, S.; Satyro, M. A.; Marriott, R. A. Screening ionic liquids as candidates for separation of acid gases: solubility of hydrogen sulfide, methane, and ethane. *AIChE J.*

2013, 59(8), 2993-3005 DOI 10.1002/aic.14081

(34) Jalili, A. H.; Shokouhi, M.; Maurer, G.; Hosseini-Jenab, M. Solubility of CO_2, and H_2S in the ionic liquid 1-ethyl-3-methylimidazolium tris(pentafluoroethyl)trifluorophosphate. *J. Chem. Thermodyn.* **2013**, 67(6), 55-62 DOI 10.1016/j.jct.2013.07.022.

(35) Peng, D. L.; Zhang, J. N.; Cheng, H. Y.; Chen, L. F.; Qi, Z. W. Computer-aided ionic liquid design for separation processes based on group contribution method and COSMO-SAC model. *Chem. Eng. Sci.* **2016**, 159, 58-68 DOI 10.1016/j.ces.2016.05.027.

(36) Farahipour, R.; Mehrkesh, A.; Karunanithi, A. T. A systematic screening methodology towards exploration of ionic liquids for CO_2 capture processes. *Chem. Eng. Sci*. **2016**, 145, 126-132 DOI 10.1016/j.ces.2015.12.015.

(37) Zhao, Y. S.; Gani, R.; Afzal, R. M.; Zhang, X. P.; Zhang, S. J. Ionic liquids for absorption and separation of gases: an extensive database and a systematic screening method. *AIChE J.* **2017**, 63, 1353-1367 DOI 10.1002/aic.15618.

(38) Zhang, J. N.; Qin, L.; Peng, D. L.; Zhou, T.; Cheng, H. Y.; Chen, L. F.; Qi, Z. W. COSMO-descriptor based computer-aided ionic liquid design for separation processes: part II: task-specific design for extraction processes. *Chem. Eng. Sci.* **2017**, 162, 364-374 DOI 10.1016/j.ces.2016.12.023.

(39) Valencia-Marquez, D.; Flores-Tlacuahuac, A.; Vasquez-Medrano, R. An optimization approach for CO2 capture using ionic liquids. *J. Cleaner Pro.* **2016**, 168, 1652-1667 DOI 10.1016/j.jclepro.2016.11.064.

(40) Zhang, Y. Y.; Ji, X. Y.; Xie, Y. J.; Lu, X. H. Screening of conventional ionic liquids for carbon dioxide capture and separation. *Appl. Energy* **2016**, 162, 1160-1170 DOI 10.1016/j.apenergy.2015.03.071

(41) Zhou, T.; Wang, J. Y.; Mcbride, K.; Sundmacher, K. Optimal design of solvents for extractive reaction processes. *AIChE J.* **2016**, 62(9), 3238-3249 DOI 10.1002/aic.15360.

(42) Lazzús, J. A. A group contribution method to predict the melting point of ionic liquids. *Fluid Phase Equilib.* **2012**, 313, 1-6 DOI 10.1016/j.fluid.2011.09.018.

(43) Paduszyński, K.; Domańska, U. Viscosity of ionic liquids: an extensive database and a new group contribution model based on a feed-forward artificial neural network. *J. Chem. Inf. Model.* **2014**, 54, 1311-1324. DOI 10.1021/ci500206u.

(44) Delley, B. An all-electron numerical method for solving the local density functional for polyatomic molecules. *J. Chem. Phys.* **1990**, 92, 508-517 DOI 10.1063/1.458452.

(45) Muldoon, M. J.; Aki, S. N.; Anderson, J. L.; Dixon, J. K.; Brennecke, J. F. Improving carbon dioxide solubility in ionic liquids. *J. Phys. Chem. B.* **2017**, 111, 9001-9009 DOI 10.1021/jp071897q.

(46) Yokozeki,A.; Shiflett, M. B.; Junk, C. P.; Grieco, L. M.; Foo, T. Physical and chemical absorptions of carbon dioxide in room-temperature ionic liquids. *J. Phys. Chem. B*. **2008**, 112, 16654–16663 DOI 10.1021/jp805784u.

(47) Chen, Y.; Han, J.; Wang, T.; Mu, T. Determination of absorption rate and capacity of CO_2 in ionic liquids at atmospheric pressure by thermogravimetric analysis. *Energy Fuels* **2011**, 25, 5810– 5815 DOI 10.1021/ef201519g.

(48) Cabaço, M. I.; Besnard, M.; Danten, Y.; Coutinho, J. A. Solubility of CO_2 in 1-butyl-3-methyl-imidazolium-trifluoro acetate ionic liquid studied by Raman spectroscopy and DFT investigations. *J. Phys. Chem. B*. **2011**, 115(13), 3538-50 DOI 10.1021/jp111453a.(49) Jie, X.; Chau, J.; Obuskovic, G.; Sirkar, K. K. Preliminary studies of CO_2 removal from precombustion syngas through pressure swing membrane absorption process with ionic liquid as absorbent. *Ind. Eng. Chem. Res.* **2013**, 52(26), 8783-8799 DOI 10.1021/ie302122s.

(50) Najafi-Marghmaleki, A.; Barati-Harooni, A.; Mohammadi, A. H.; Efficient estimation of acid gases (CO_2 and H_2S) absorption in ionic liquids. *Int. J. Greenhouse Gas Control* **2017**,

63, 338-349 DOI 10.1016/j.ijggc.2017.05.014.

(51) Liu, Z.; Liu, C.; Li, L. F.; Qin, W.; Xu, A. R. CO_2 separation by supported ionic liquid membranes and prediction of separation performance. *Int. J. Greenhouse Gas Control* **2016**, 53, 79-84 DOI 10.1016/j.ijggc.2016.07.041.

(52) Shiflett, M. B.; Niehaus, A. M. S.; Yokozeki, A. Separation of CO_2 and H_2S using room-temperature ionic liquid [BMIM][MeSO4]. *Fluid Phase Equilib.* **2010**, 294, 105-113 DOI 10.1021/ef900997b.

Post-print version of the paper by Jingwen Wang et al. in ACS Sustainable Chem. Eng. 2018, 6, 9, 12025-12035. **DOI:** 10.1021/acssuschemeng.8b02321

Table options

Table 1 A list of group ID, name and valence.

Table 2 Comparison of IL design results based on different objective functions.

Table 3 Top 10 ILs based on *ASDI* and comparison with literature-reported IL for the CO_2/H_2 separation process.

Table 4 Top 10 ILs based on *ASDI* and comparison with literature-reported IL for the CO_2/H_2S separation process.

Post-print version of the paper by Jingwen Wang et al. in ACS Sustainable Chem. Eng. 2018, 6, 9, 12025-12035. **DOI:** 10.1021/acssuschemeng.8b02321

Table 1

Cation Skeletons			Anions			Substituents		
ID	Name	Valence	ID	Name	Valence	ID	Name	Valence
1	Im1	1	1	BF_4	0	1	CH_3	1
2	Im13	2	2	Cl	0	2	CH_2	2
3	Im123	3	3	H_2PO_4	0	3	CH	3
4	Mp12	2	4	DMP	0	4	C	4
5	Pi12	2	5	$N(CN)_2$	0	5	HC=CH	2
6	Pyo12	2	6	$MeSO_4$	0	6	CH_2=CH	1
7	Py1	1	7	NO_3	0	7	CH_2=C	2
8	Py12	2	8	PF_6	0	8	OH	1
9	Py13	2	9	Tf_2N	0	9	O	2
10	Py14	2	10	SCN	0	10	C=O	2
11	N	4	11	OAc	0	11	CHO	1
12	P	4	12	$AlCl_4$	0	12	COOH	1
						13	CN	1
						14	F	1
						15	Cl	1
						16	Br	1

Post-print version of the paper by Jingwen Wang et al. in ACS Sustainable Chem. Eng. 2018, 6, 9, 12025-12035. **DOI:** 10.1021/acssuschemeng.8b02321

Table 2

Entry	Objective function	Range of absorption performance indices of top 10 IL candidates					Molecular weight
		H (bar)	*H′* (bar)	*1/S′*	*D′*	*ASDI* (bar)	
1	*H*	4.99 - 5.71	93.22 - 106.68	0.076 - 0.091	0.52 - 0.54	3.84 - 4.96	791 - 819
2	*H′*	6.39 - 8.75	42.59 - 56.74	0.078 - 0.091	0.49 - 0.54	1.81 - 2.58	277 - 319
3	*1/S′*	41.75 - 676.94	293.62 - 2369.31	0.017 - 0.024	0.52 - 0.61	3.06 - 26.02	154 - 310
4	*D′*	16.94 - 55.12	76.26 - 235.51	0.069 - 0.085	0.35 - 0.39	2.44 - 6.01	191 - 238
5	*ASDI*	11.81 - 15.73	60.11 - 70.57	0.032 - 0.036	0.39 - 0.46	0.89 - 1.04	196 - 238

Post-print version of the paper by Jingwen Wang et al. in ACS Sustainable Chem. Eng. 2018, 6, 9, 12025-12035. **DOI:** 10.1021/acssuschemeng.8b02321

Table 3

No	ILs	*ASDI* (bar)	*H'* (bar)	*1/S'*	*D'*	T_m (K)	η (cP)
1	[MPy13CH_2COOH][OAc]	0.013	61.99	0.00053	0.41	272.14	94.33
2	[MPy13$(CH_2)_2$COOH][OAc]	0.013	60.11	0.00053	0.41	268.38	96.3
3	[MPy14CH_2COOH][OAc]	0.017	65.49	0.00054	0.47	272.14	94.33
4	[EPy13CH_2COOH][OAc]	0.017	68.23	0.00054	0.45	268.38	97.48
5	[MPy13COOH][OAc]	0.018	70.07	0.00055	0.46	275.9	90.53
6	[EPy13$(CH_2)_2$COOH][OAc]	0.018	66.47	0.00056	0.47	264.62	98.49
7	[CH_2COOHPy13C_2H_5][OAc]	0.020	78.17	0.00056	0.45	268.38	97.48
8	[PPy13COOH][OAc]	0.020	72.67	0.00058	0.47	268.38	97.48
9	[PPy13CH_2COOH][OAc]	0.021	71.29	0.00061	0.49	264.62	98.49
10	[C_2H_5COOHPy13C_2H_5][OAc]	0.022	84.49	0.00056	0.47	260.86	98.72
Ref.	[BMIM][TfO]	0.15	244.16	0.0011	0.54	326.13	89.23

Post-print version of the paper by Jingwen Wang et al. in ACS Sustainable Chem. Eng. 2018, 6, 9, 12025-12035. **DOI:** 10.1021/acssuschemeng.8b02321

Table 4

No	ILs	*ASDI* (bar)	*H'* (bar)	*1/S'*	*D'*	T_m (K)	η (cP)
1	$[PyCC_7C_9C_{17}][AlCl_4]$	3.56	119.91	0.052	0.53	219.42	21.37
2	$[PyCC_1C_{14}C_{18}][AlCl_4]$	3.57	119.15	0.053	0.53	219.42	21.37
3	$[PyCC1C_6C_{26}][AlCl_4]$	3.77	123.47	0.054	0.53	219.42	21.37
4	$[PyCC_1C_{22}C_{10}][AlCl_4]$	4.08	129.85	0.056	0.53	219.42	21.37
5	$[PyCC_3C_{11}C_{20}][AlCl_4]$	4.23	119.73	0.054	0.53	219.42	21.37
6	$[PyCH_2{=}CC_2CC_1C_2C_{29}][AlCl_4]$	4.25	131.08	0.057	0.53	209.47	21.16
7	$[PyCH_2{=}CC_2CC_1C_1C_{30}][AlCl_4]$	4.43	126.16	0.054	0.53	219.42	21.37
8	$[PyCC_6C_{11}C_{16}][AlCl_4]$	4.62	138.20	0.059	0.53	209.47	21.16
9	$[PyCC_5C_{24}C_4][AlCl_4]$	4.68	131.95	0.055	0.53	219.42	21.37
10	$[PyCC_6C_9C_{18}][AlCl_4]$	4.75	133.60	0.055	0.53	219.42	21.37
Ref.	$[BMIM][MeSO_4]$	8.64	209.95	0.071	0.57	306.96	184.17

Post-print version of the paper by Jingwen Wang et al. in ACS Sustainable Chem. Eng. 2018, 6, 9, 12025-12035. **DOI:** 10.1021/acssuschemeng.8b02321

Figure captions

Figure 1 Strategy of the proposed CAILD method.

Figure 2 Deviation of thermodynamic model for Henry's law constants (bar): (a) comparison between COSMO-GC-IL-inputted and DMol^3-inputted calculations; (b) comparison between COSMO-GC-IL-inputted calculations and experimental data.

Figure 3 Evolution of objective function value of (a) *H* and (b) *ASDI* vs. the number of generations for the CO_2/N_2 separation case study.

Figure 4 Comparison of the absorption performances (a) *H′*; (b) *1/S′*; (c) *D′*, and (d) *ASDI* of the top 10 designed ILs with the literature-reported $[P_{4,4,4,10}]$[DCA] for the flue gas separation case study.

Figure 5 Evolution of objective function value vs. the number of generations for the CO_2/H_2 separation case study.

Figure 6 Evolution of objective function value vs. the number of generations for the CO_2/H_2S separation case study.

Figure 7 σ-Profiles of (a) gas components, (b) the cations, and (c) anions in the optimal ILs designed for the three CO_2 separation tasks.

Post-print version of the paper by Jingwen Wang et al. in ACS Sustainable Chem. Eng. 2018, 6, 9, 12025-12035. **DOI:** 10.1021/acssuschemeng.8b02321

Figure 1

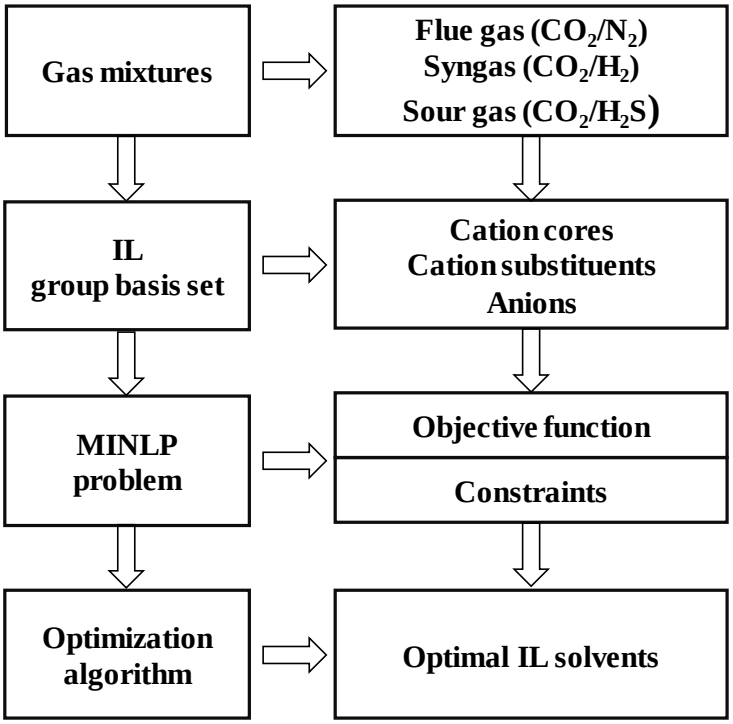

Post-print version of the paper by Jingwen Wang et al. in ACS Sustainable Chem. Eng. 2018, 6, 9, 12025-12035. **DOI:** 10.1021/acssuschemeng.8b02321

Figure 2

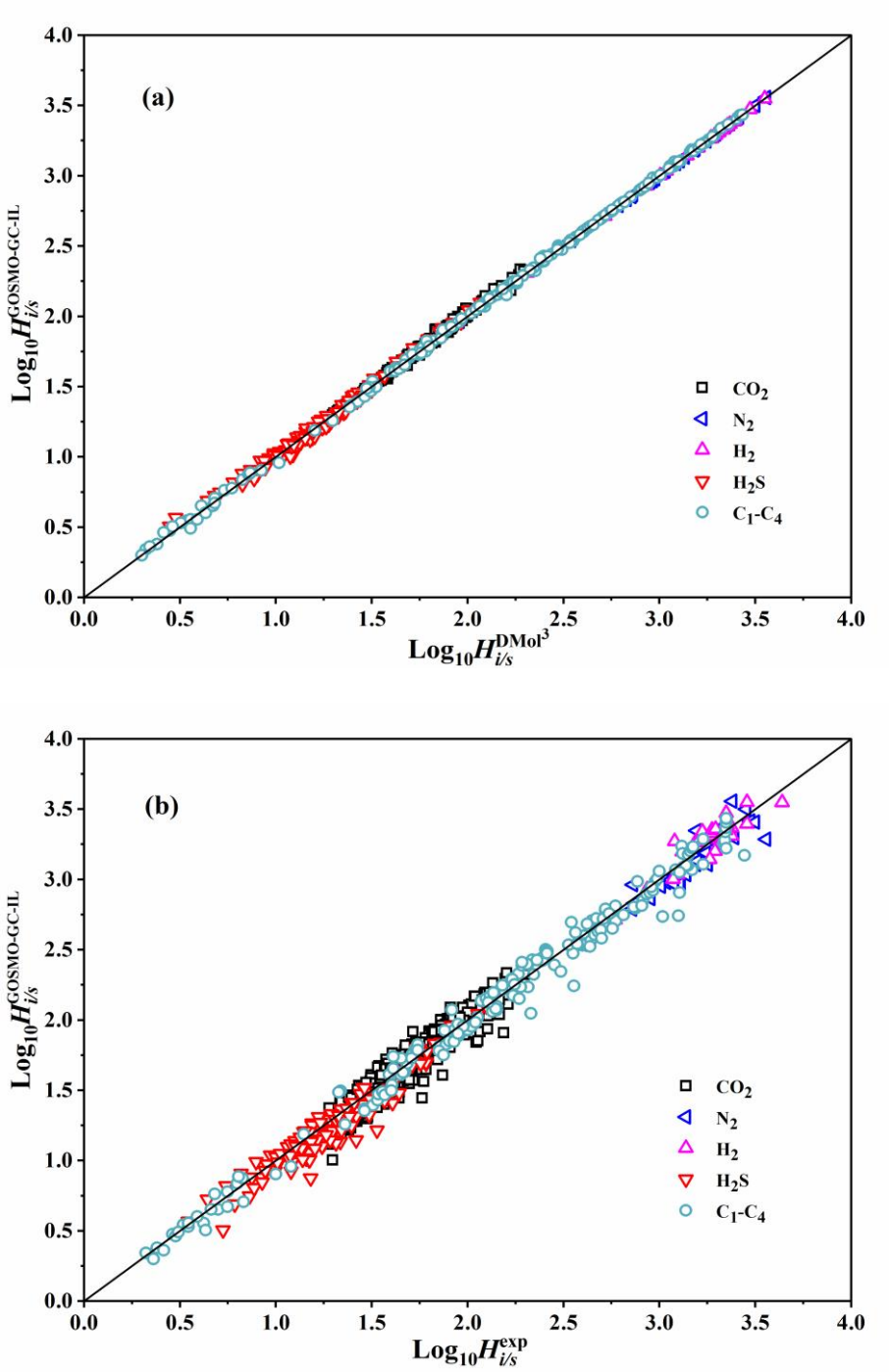

Post-print version of the paper by Jingwen Wang et al. in ACS Sustainable Chem. Eng. 2018, 6, 9, 12025-12035. **DOI:** 10.1021/acssuschemeng.8b02321

Figure 3

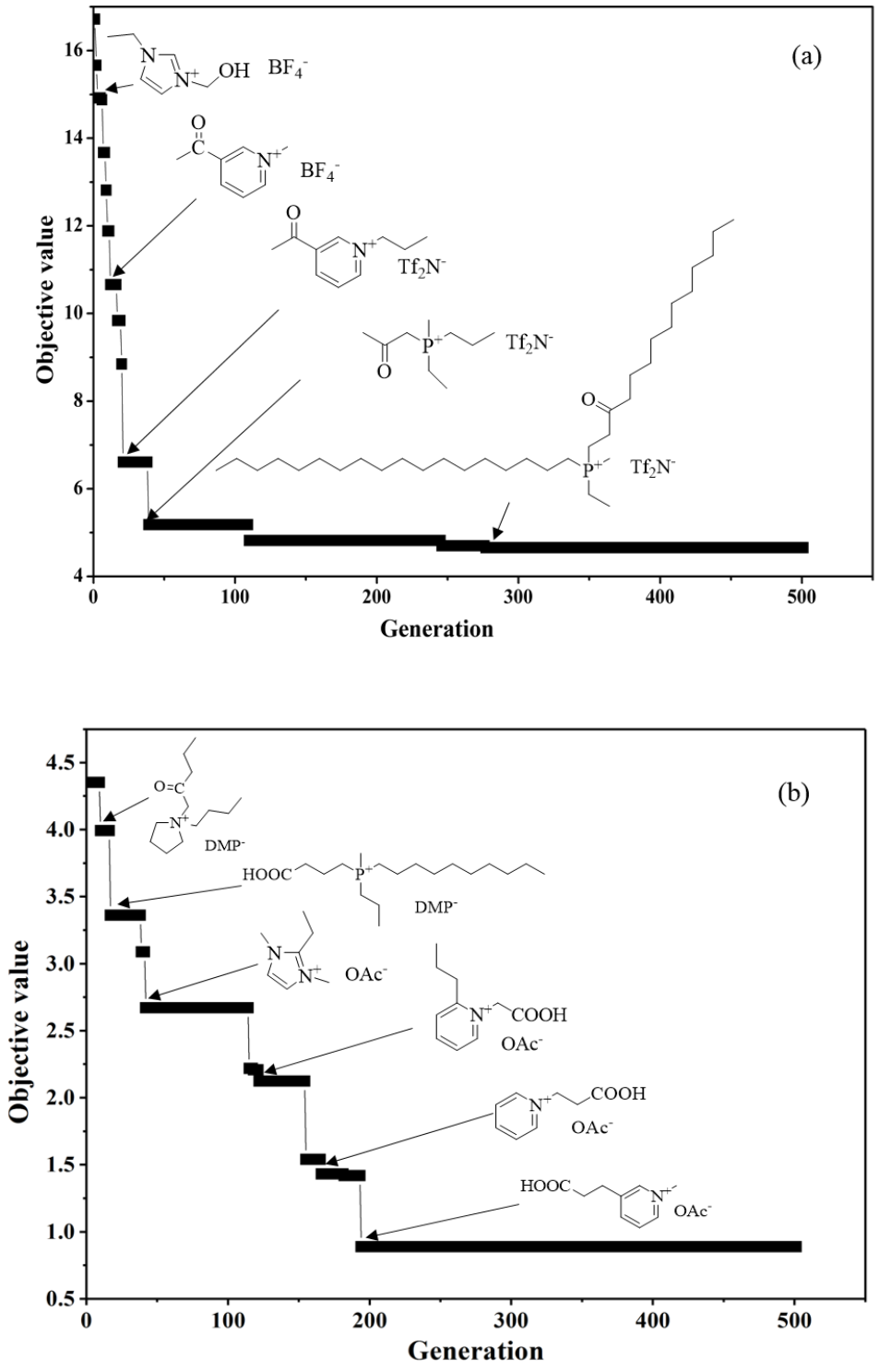

Post-print version of the paper by Jingwen Wang et al. in ACS Sustainable Chem. Eng. 2018, 6, 9, 12025-12035. **DOI:** 10.1021/acssuschemeng.8b02321

Figure 4

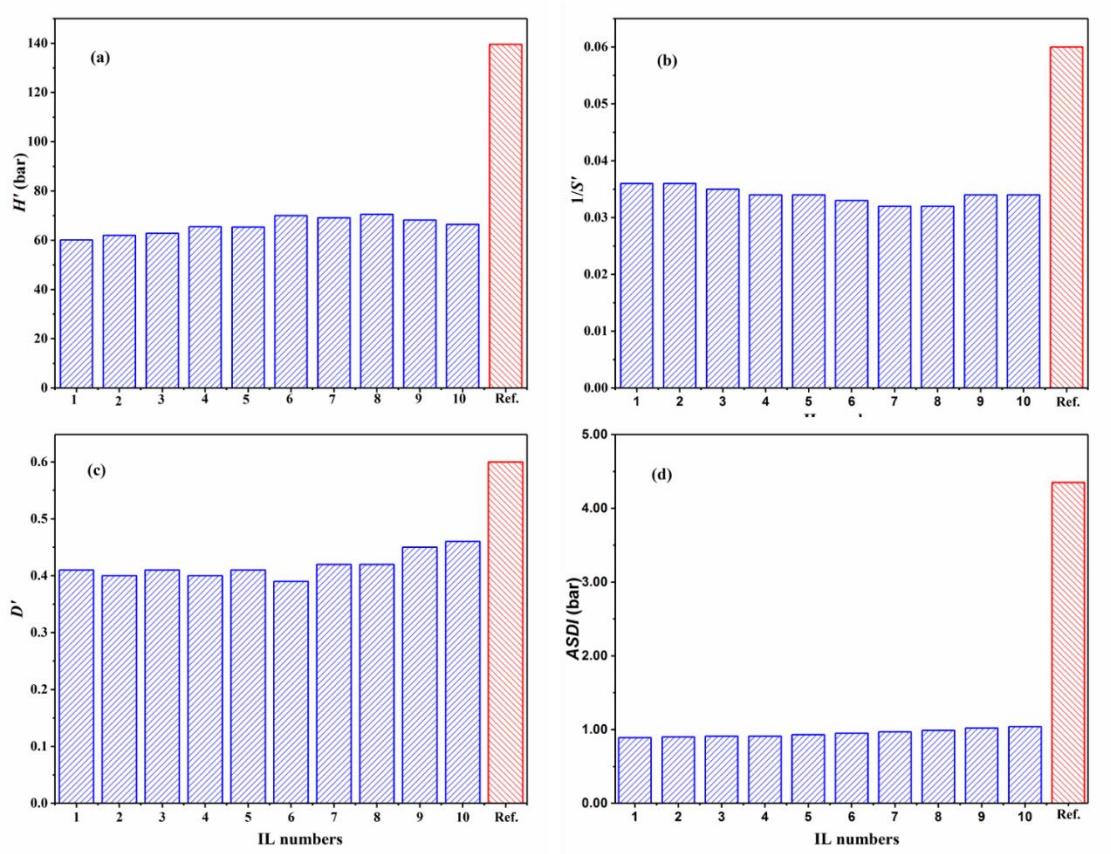

Post-print version of the paper by Jingwen Wang et al. in ACS Sustainable Chem. Eng. 2018, 6, 9, 12025-12035. **DOI:** 10.1021/acssuschemeng.8b02321

Figure 5

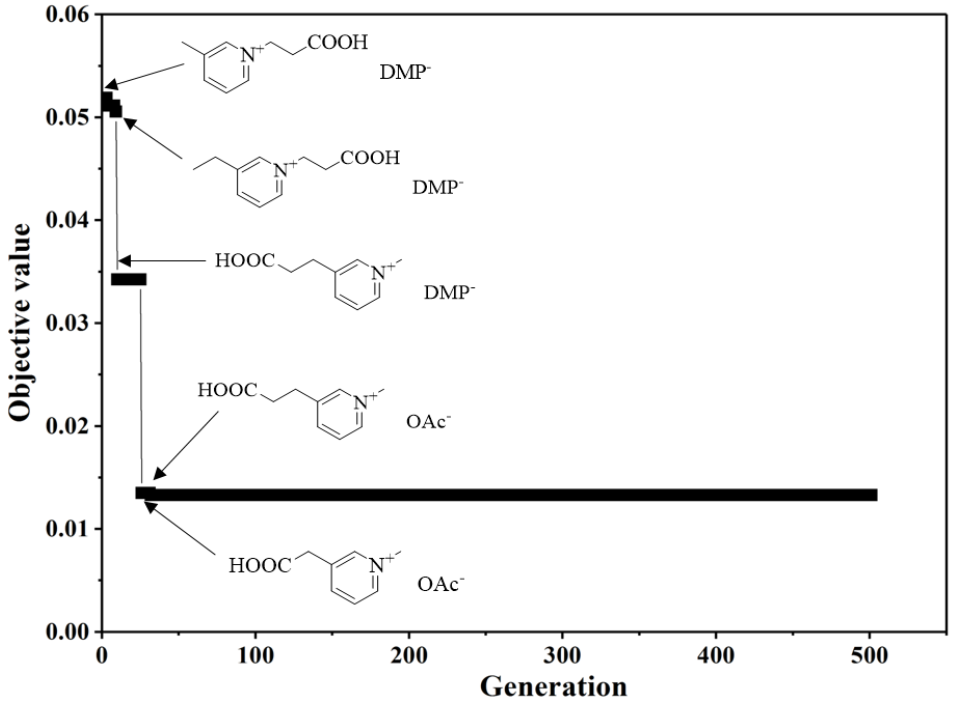

Post-print version of the paper by Jingwen Wang et al. in ACS Sustainable Chem. Eng. 2018, 6, 9, 12025-12035. **DOI:** 10.1021/acssuschemeng.8b02321

Figure 6

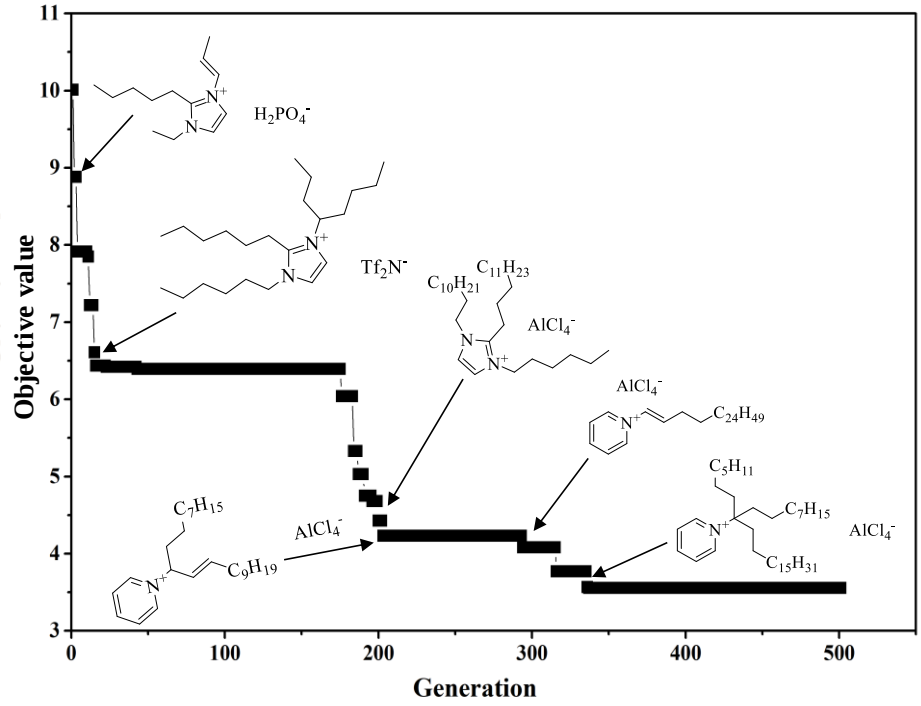

Post-print version of the paper by Jingwen Wang et al. in ACS Sustainable Chem. Eng. 2018, 6, 9, 12025-12035. **DOI:** 10.1021/acssuschemeng.8b02321

Figure 7

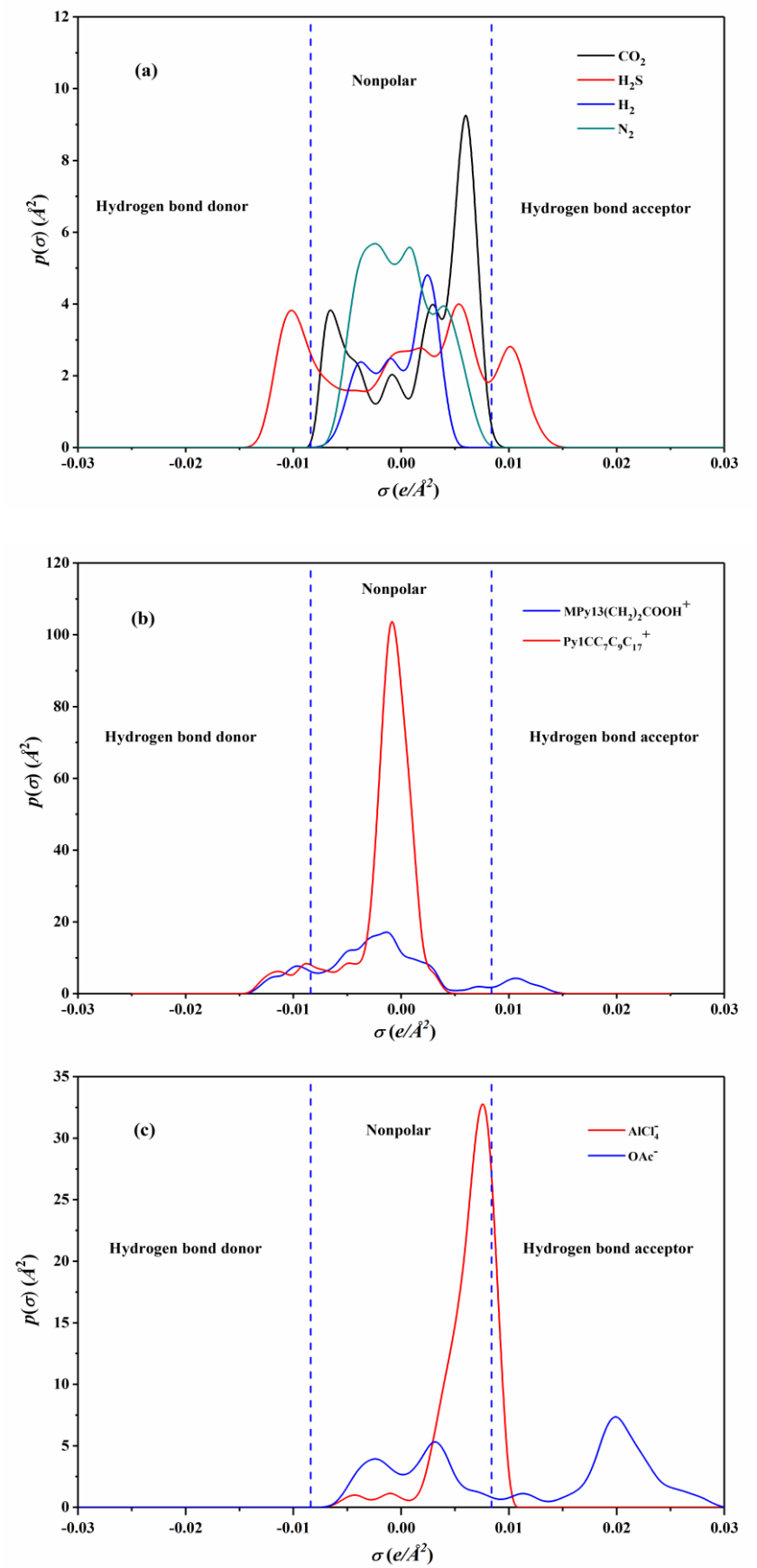

Post-print version of the paper by Jingwen Wang et al. in ACS Sustainable Chem. Eng. 2018, 6, 9, 12025-12035. **DOI:** 10.1021/acssuschemeng.8b02321

Graphic for manuscript:

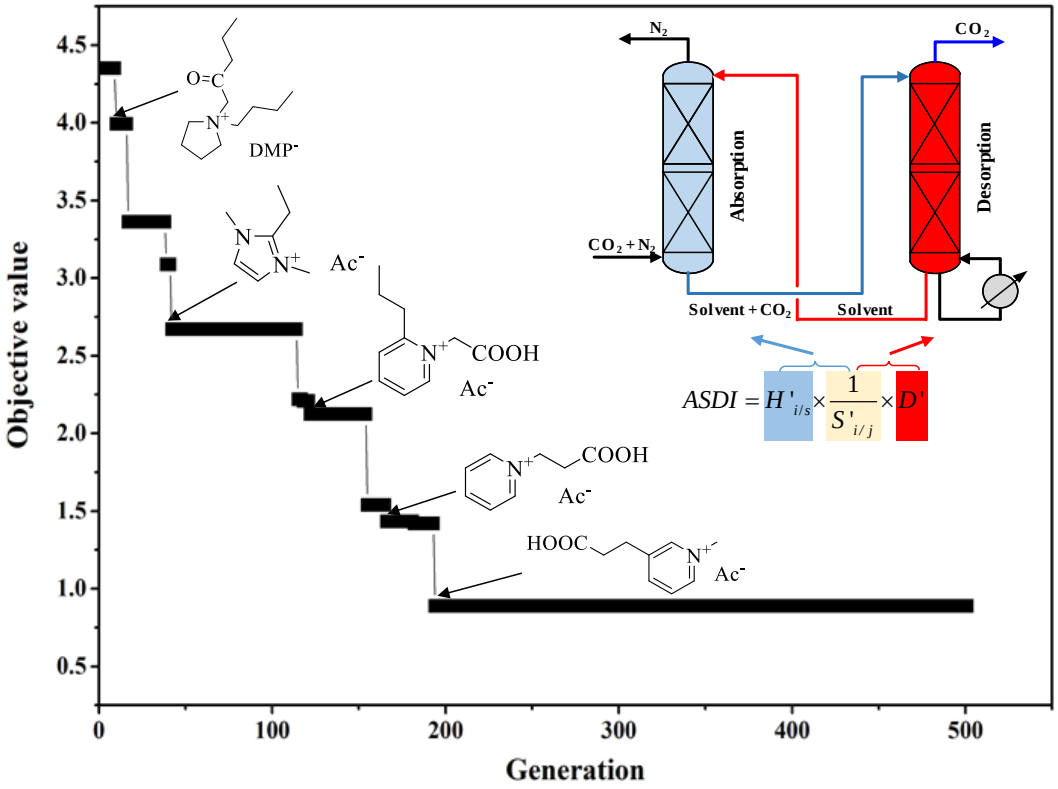

A mass-based Absorption-Selectivity-Desorption index (*ASDI*) is proposed as the objective function and optimized by solving the mixed-integer nonlinear programming (MINLP) problems.